

Optically Transparent Dual-Band Frequency Selective Surfaces for Smart Surfaces

S. Can¹, K.Y. Kapusuz^{2,3}, A.E. Yilmaz¹

¹Department of Electrical and Electronics Engineering, Ankara University, Ankara, Turkey

²Department of Information Technology, IDLab/EM Group, Ghent University/imec, Ghent, Belgium

³ Univ. Rennes, CNRS, IETR (Institut d'Electronique et des Technologies du numéRique), Rennes, France
sultancan@ankara.edu.tr, kamilyavuz.kapusuz@ugent.be, aeyilmaz@eng.ankara.edu.tr

Abstract – Optically transparent dual-band frequency selective surfaces (FSSs) are promising candidates to address the specific design challenges posed by the Internet of Things (IoT). This contribution demonstrates their potential by discussing different configurations of the two FSS designs on an innovative optically transparent surface material. First, a single-layer dual-band FSS is presented. Then, in the second design, the modular multi-layer technique is applied to achieve dual-band performance, enabling invisible integration into optically transparent polyvinyl chloride (PVC) surface material. The transparency, compactness, integrability, and high-performance dual-band stability of both designs in different operating conditions make them ideal for IoT applications.

I. INTRODUCTION

In the context of multitude communication of Internet of Things (IoT), optically transparent multiband or wide-band frequency selective surfaces (FSSs) are desired for seamless integration into light-permeable surfaces [1]. Meanwhile, polarization (in)sensitivity, even for large oblique incidence angles, must be maintained to make provision for rotation in polarization by surrounding materials [2]. Moreover, for mass production, a cost-effective and robust fabrication process is needed.

In this paper, we describe a new cost-effective manufacturing technology to realize dual-band FSSs for IoT. Specially, we discussed two novel FSS designs based on this technology, which can be part of high-performance optically transparent smart surfaces. All the designed FSSs were optimized for the operation of sub-6 GHz.

To manufacture optically transparent FSSs, numerous solutions have been investigated by exploiting diverse fabrication methodologies [3-4]. Thin-film technique with transparent conductive material, such as silver-coated polyester film (AgHT), indium tin oxide (ITO), or fluorine-doped tin oxide (FTO) are commonly preferred [3]. Even though these technologies are promising solutions to obtain high optical transparency, the process is expensive, and they suffer from losses due to surface resistance. Therefore, they are not ideal for large surfaces. In [4], copper grids are used as a conductive material. Yet, since the traces in the design are quite thick, it makes the structure semitransparent. In contrast, our approach complies with a wide variety of everyday surfaces with high optical transparency without requiring a specific chemical process.

II. REALIZATION OF OPTICALLY TRANSPARENT FSSS

Realizing the FSSs by exploiting the materials available in everyday objects is interesting for the IoT since this yields a significant cost and area reduction [5]. Initially, RF material properties are characterized by exploiting two-line method [6] as the electromagnetic characteristics of these unconventional RF materials vary in frequency selective manner and cause losses from batch-to-batch. Then, special attention is employed to keep the optical blockage bare minimum while imposing the performance maximum.

The proposed surfaces consist of dielectric and conductive layers. The main purpose of the dielectric layers is to provide support to the conducting FSS patterns. To allow the visible electromagnetic fields to pass through the surface, optically transparent 1.48-mm-thick polyvinyl chloride (PVC) material ($\epsilon_r = 2.77$) is exploited as a dielectric layer. To enable the cost-effective realization of high-performance FSS, conducting patterns are implemented

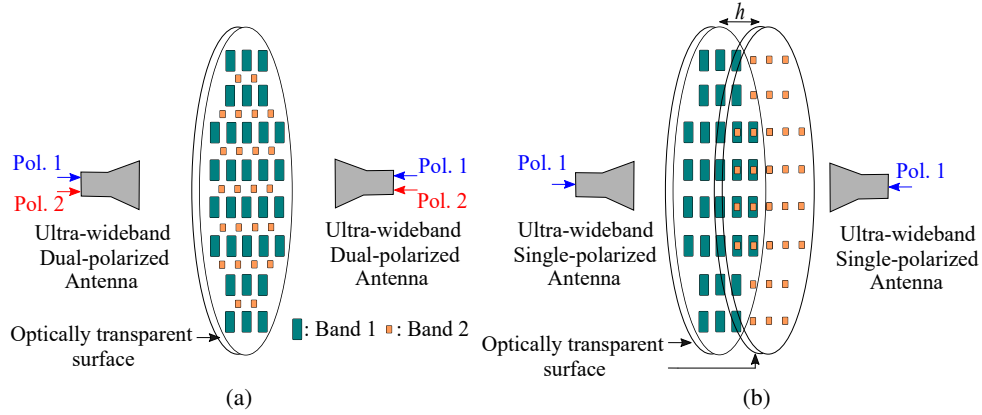


Fig. 1: Optically transparent dual-band FSSs with two different configurations: (a) single-layer and (b) multi-layer.

on conductive tape by HP laserjet P1005 printer. Next, they are cut out by scissors and glued through predefined positions and periodicity on the optically transparent PVC surface. Consequently, by judiciously patterning the different shapes and sizes of these conductive patterns, the functionality of the FSS is defined.

III. OPTICALLY TRANSPARENT DUAL-BAND FSSS

A. Single-Layer Configuration

The first proposed FSS is depicted in Fig. 1(a). To achieve low profile design, a single layer configuration is employed [7]. To operate at two separate bands with polarization insensitive characteristics while providing high optical transparency, two independent ring resonators with different dimensions are placed in a single unit cell. To minimize the coupling between two bands, two types of rings corresponding to each band are arranged in an interlaced array arrangement, as shown in Fig. 2(a).

B. Multi-Layer Configurations

The second proposed dual-band FSS is presented in Fig. 1(b). A multi-layer topology is exploited to overcome the drawbacks of single-layer configurations (larger optical blockage, narrower bandwidth) while preserving the advantages of planar technology, being cost-effective fabrication and light weight [8]. Dual-band characteristic is achieved by stacking both different sized square ring resonators and the same sized square ring resonators with different sized capacitive gaps in each layer, as shown in Fig. 2(b). Notice that diverse selection of layer-to-layer spacing h , optical transparency and coupling between each band can be controlled.

IV. EXPERIMENTAL VALIDATION

The fabricated prototypes of the single and multilayer dual-band FSSs are depicted in Fig. 2(a) and Fig. 2(b), respectively. The S-parameters of the single-layer topology was validated by means of an Rohde & Schwarz ZVL13 Vector Network Analyzer (VNA) and two Rohde & Schwarz HF907 double ridge horn antennas in a semi-anechoic chamber, whereas a WR-229 waveguide and the same VNA were exploited for the characterization of multilayer topology. For adequate comparison between simulation and measurement results, horn antennas and waveguide-to-coaxial probe transitions were de-embedded.

The measured transmission coefficients for both designs are shown in Fig. 2, along with the full-wave simulation results. They are in good agreement considering the inhomogeneous RF characteristics of everyday materials and various sources of fabrication tolerances. As it is seen, an excellent dual-band frequency selection is achieved from both of the prototypes. Moreover, Fig. 2(a) shows that transmission coefficients of both linear polarization states at 2.5 GHz and 5.1 GHz are identical owing to the geometrical and modal azimuthal symmetry of the resonators while maintaining a transparency level of 77.5%. Yet, above 3 GHz, additional loss is observed in the inhomogeneous dielectric material. On the other hand, frequency control of each frequency band is shown in Fig. 2(b) by stacking

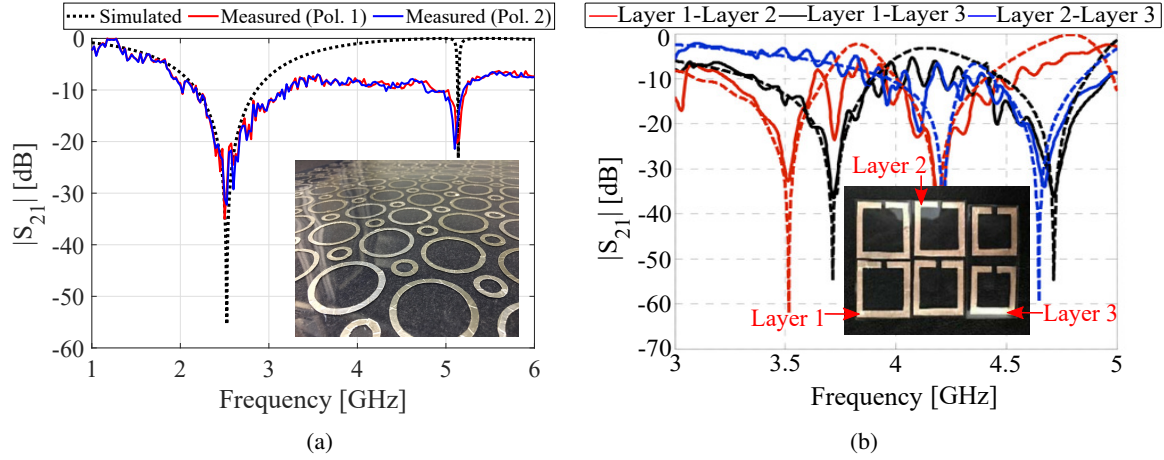


Fig. 2: Fabricated prototypes and measurement results of (a) single and (b) multi-layer topologies. (---: Simulation. —: Measurement.)

different sized conductor patterns on dielectric layers. For the combination of stacked Layer 1 and Layer 2, the transmission coefficients below -30 dB are achieved at 2.5 GHz and 5.1 GHz, whereas 3.7 GHz and 4.7 GHz bands are filtered out by stacking Layer 1 and Layer 3. Finally, for the combination of stacked Layer 2 and Layer 3, 4.1 GHz and 4.67 GHz bands are suppressed.

V. CONCLUSION

The printing technology is combined with innovative optically transparent material to realize two different cost-effective high-performance, dual-band FSS designs to enable invisible integration in an IoT environment. More specifically, two strategies were discussed to demonstrate the merits and potential of this design approach: a single layer dual-band FSS and a modular multi-layer dual-band FSS for seamless integration into light-permeable surfaces. Measurements have been performed and demonstrate excellent performance, proving the potential of our approach for IoT.

ACKNOWLEDGEMENT

Sultan Can would like to thank the Ankara University Scientific Research Fund (BAP)-BAP grant no: 21O0443002. Kamil Yavuz Kapusuz would like to thank the Research Foundation Flanders (FWO) for the grant V43420N.

REFERENCES

- [1] N.B. M. Nafis, M. Himdi, M. K. A. Rahim, O. Ayop, and R. Dewan, "Optically transparent tri-wideband mosaic frequency selective surface with low cross-polarisation," *Materials*, vol. 15, no. 2, pp. 622, Jan. 2022.
- [2] Y. Yang, W. Li, K. N. Salama, and A. Shamim, "Polarization insensitive and transparent frequency selective surface for dual band GSM shielding," *IEEE Trans. Antennas Propag.*, vol. 69, no. 5, pp. 2779–2789, May 2021.
- [3] A. A. Dewani, S. G. O'Keefe, D. V. Thiel, and A. Galehdar, "Window RF shielding film using printed FSS," *IEEE Trans. Antennas Propag.*, vol. 66, no. 2, pp. 790–796, Feb. 2018.
- [4] F. Bagci, C. Mulazimoglu, S. Can, E. Karakaya, A. E. Yilmaz, and B. Akaoglu, "A glass based dual band frequency selective surface for protecting systems against WLAN signals," *AEU-International Journal of Electronics and Communications*, vol. 82, pp. 426–434, Dec. 2017.
- [5] S.-H. Lee, M.-S. Kim, J.-K. Kim, and I.-P. Hong, "Design of security paper with selective frequency reflection characteristics," *Sensors*, vol. 18, no. 7, pp. 2263, July 2018.
- [6] F. Declercq, H. Rogier, and C. Hertleer, "Permittivity and loss tangent characterization for garment antennas based on a new matrix-pencil two-line method," *IEEE Trans. Antennas Propag.*, vol. 56, no. 8, pp. 2548–2554, Aug. 2008.
- [7] S. Can, K.Y. Kapusuz, and A.E. Yilmaz, "A dual-band polarization independent FSS having a transparent substrate for ISM and Wi-Fi shielding," *Microw. and Optical Technol. Lett.*, vol. 59, no. 9, pp. 2249–2253, Sept. 2017.
- [8] S. Can, K.Y. Kapusuz, and A.E. Yilmaz, "Optically transparent frequency selective surface for ultra-wideband applications," *Microw. and Optical Technol. Letters*, vol. 59, no. 12, pp. 3197–3201, Dec. 2017.